

Comparison of the dynamic responses of Gülburnu Highway Bridge using single and triple concave friction pendulums

Muhammet Yurdakul^{*1}, Sevket Ates^{2b} and Ahmet Can Altunisik^{2c}

¹Bayburt University, Department of Civil Engineering, 69000, Bayburt, Turkey

²Karadeniz Technical University, Department of Civil Engineering, 61080 Trabzon, Turkey

(Received March 13, 2014, Revised May 26, 2014, Accepted June 9, 2014)

Abstract. The main object of this study is to determine and compare the structural behavior of base isolated long span highway bridge, Gülburnu Highway Bridge, using single concave friction pendulum (SCFP) and triple concave friction pendulum (TCFP). The bridge is seismically isolated in the design phase to increase the main period and reduce the horizontal forces with moments using SCFP bearings. In the content of the paper, firstly three dimensional finite element model (FEM) of the bridge is constituted using project drawings by SAP2000 software. The dynamic characteristics such as natural frequencies and periods, and the structural response such as displacements, axial forces, shear forces and torsional moments are attained from the modal and dynamic analyses. After, FEM of the bridge is updated using TCFP and the analyses are performed. At the end of the study, the dynamic characteristics and internal forces are compared with each other to extract the TCFP effect. To emphasize the base isolation effect, the non-isolated structural analysis results are added to graphics. The predominant frequencies of bridge non-isolated, isolated with SCFP and isolated with TCFP conditions decreased from 0.849Hz to 0.497Hz and 0.338Hz, respectively. The maximum vertical displacements are obtained as 57cm, 54cm and 44cm for non-isolated, isolated with SCFP and isolated with TCFP conditions, respectively. The maximum vertical displacement reduction between isolated with TCFP bearing and isolated with SCFP bearing bridge is %23. Maximum axial forces are obtained as 60619kN, 18728kN and 7382kN, maximum shear forces are obtained as 23408kN, 17913kN and 16249kN and maximum torsional moments are obtained as 24020kNm, 7619kNm and 3840kNm for non-isolated, isolated with SCFP and isolated with TCFP conditions, respectively.

Keywords: dynamic characteristics; finite element model; long span highway bridge; single concave friction pendulums; triple concave friction pendulums

1. Introduction

Among all types of civil engineering structures, long span highway bridges attract the greatest interest for studies of structural performance by the academic researchers (Brownjohn et al. 2010). Dynamic characteristics (natural frequencies, mode shapes and damping ratios) and internal forces (displacements, axial forces, shear forces and torsional moments) can be selected as comparison

^{*a}Corresponding author, Ph.D. Student, E-mail: myurdakul@bayburt.edu.tr

^bAssociate Professor, E-mail: sates@ktu.edu.tr

^cAssociate Professor, E-mail: ahmetcan@ktu.edu.tr

parameters to evaluate the structural performance. In the last two decades, seismic isolation has been considered as reliable and cost effective technology to alleviate the risks of seismic damages to highway bridges.

Seismic isolation systems generally make structure resistant to earthquake excitations. It is meant to shift the natural period of a bridge structure in such a way that the dominant frequency of the earthquake ground acceleration can safely be avoided to safeguard it against seismic damages (Rahman and Shahria 2013). In addition, the inherently occupied damping property and energy dissipation mechanism prevents the bridge system from over displacement (Kelly 1997). As a result of these positive effects, the seismic isolation techniques have been rapidly a widespread application. Seismic isolation systems are easy to install new and need to retrofitting structures.

There are two types of isolation systems in terms of behavior which are elastomeric bearing and bearing based on sliding. The elastomeric bearing systems included lead use rubber for restoring force and hysteretic damping of lead for energy dissipation. Important feature of the bearings based on sliding bearings is energy dissipation related to velocity dependent on friction between stainless steel plates (Tsopelas and Constantinou 1996). Sliding bearings use their curvature surfaces to generate the restoring forces from weight of structure on isolation systems.

In the literature, there are some studies related to structural performance evaluation of base isolated long span highway bridges. Hyakuda et al. (2001) exhibited the performance of seismically isolated structures with double concave friction pendulums (DCFP) bearings in Japan. Dicleli and Mansour (2003) studied about the retrofitting of typical seismically vulnerable bridges isolated with SCFP bearings in the State of Illinois. Hamidi et al. (2003) introduced a new base isolation system similar to SCFP, namely the sliding concave foundation (SCF). In this system, large radius of foundation curvature represented to pendulum behavior. Jangid (2004) examined into seismically isolated bridge with lead rubber bearings using two lateral earthquake excitations. Dicleli et al. (2005) displayed to soil-structure interaction effect on the earthquake response of seismic isolated bridges. Fenz and Constantinou (2006) investigated to DCFP bearings with the same and different radius of curvatures and coefficients friction. Madhekar and Jangid (2010) evaluated to a highway bridge isolated with variable friction pendulum system (VFPS) in California and analyzed them using six ground motions acceleration records. Marin-Artieda and Whittaker (2010) practiced on XY friction pendulum bearings installed on a highway bridge. This bearing can be called as modified friction pendulum consists of two orthogonal stainless steel rails with opposing concave surfaces and a connector withstand tensile forces, permits independent sliding in the two orthogonal directions. Soni et al. (2011) described a mathematical model and force-displacement relationships of double variable frequency pendulum isolator (DVFPI). Behavior of this isolator is examined by varying its geometry and coefficient of friction of the sliding surfaces. Ates and Constantinou (2011) performed on a long span curved highway bridge isolated with DCFP placed between the deck and the piers. It can be seen from the literature that there is no enough studies about determination and comparison of structural behavior of base isolated long span highway bridge using SCFP and TCFP bearings.

The main object of this study is to determine and compare the structural behavior of base isolated long span highway bridge using SCFP and TCFP. Gülburnu long span highway bridge is seismically isolated in the design phase selected as an application. Finite element analyses are performed to non-isolated, SCFP and TCFP bearings conditions. The dynamic characteristics and internal forces are compared with each other to extract the TCFP effect.

2. Triple concave friction pendulum bearing

The TCFP bearing is consisted of two facing concave stainless steel surfaces coated with teflon separated by a placed slider assembly (Fig. 1). R_i is the radius of curvature of surface i , h_i is the radial distance between the pivot point and surface i and μ_i is the coefficient of friction at the sliding surface i , d_i is the displacement capacity of the surface i . Outer concave plates have effective radii $R_{eff1}=R_1-h_1$ and $R_{eff4}=R_4-h_4$.

The articulated slider assembly consists of two concave plates separated by a rigid slider. Though the innermost slider is rigid, the assembly as a whole has the capability to rotate to accommodate differential rotations of the top and bottom plates. The friction coefficients on these concave plates are μ_1 and μ_4 . The inner concave plates have effective radii $R_{eff2}=R_2-h_2$ and $R_{eff3}=R_3-h_3$. Additionally, these surfaces are also coated with Teflon. The friction coefficients on these concave plates are μ_2 and μ_3 . This leads to motion of slider between up and down stainless of steel surfaces of slide plates. The concave surfaces of TCFP bearing are chosen to become sequentially active at different earthquake strengths.

The main principle of TCFP bearing, three effective radii of curvature and three friction coefficients are selected to optimize performance for different strengths and frequencies of earthquake excitations. This allows for maximum design flexibility to accommodate both moderate and extreme motions, including near-fault excitations. This reduces construction costs of the structures. Unlike the SCFP and DCFP, there is no mechanical defined constraint at the pivot point location in the TCFP bearing. (Fenz and Constantinou 2008a). As the ground excitations become stronger, the bearing displacements increase. Differently to SCFP bearing, TCFP bearing lets simultaneous sliding on multiple concave surfaces. The plan dimensions of the TCFP bearing are approximately 60% that of the equivalent SCFP bearing.

TCFP bearing system is important for lengthens period of structure. In this study, TCFP bearing is used on a bridge. Besides this, TCFP bearing is used on different type of buildings and different standing of airport structure (under roof or under column), and LNG tanks.

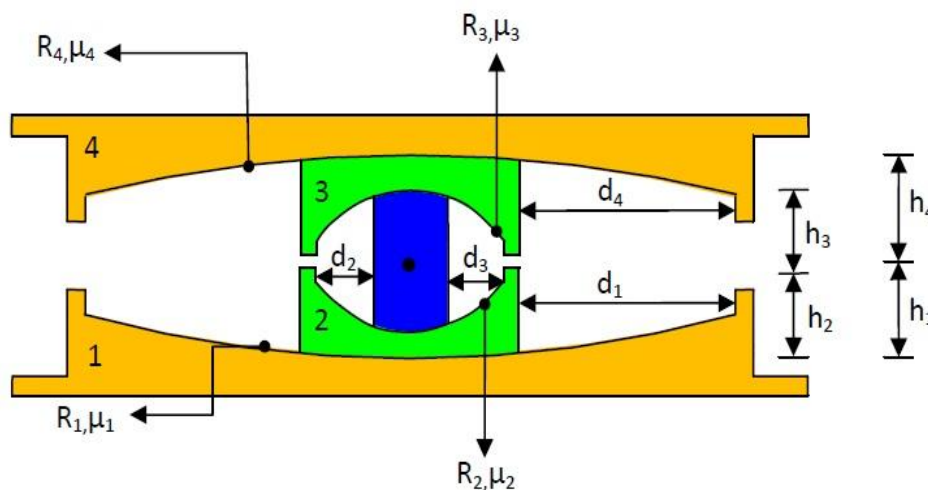


Fig. 1 The cross-section of the TCFP bearing and its definition of dimensions

2-1 Series Model of the TCFP Bearing

There are practicable no hysteresis rules or nonlinear elements present in structural program that can be used triple friction model in series model for response history analysis. Series model consists of linear element which can be used in present software structural analysis program. But, the TCFP bearing is not exactly like a model organized as a three SCFP bearing in series model although it is similar. Series model is favored because of their implementation in available commercial structural analysis program such as SAP2000 (SAP2000 2007). It has nonlinear elements modelling rigid linear behavior of the SCFP bearings. However, one behavioral event is preventing correctly modelling the TCFP bearing as a three SCFP bearing. This event is there is no sliding simultaneous on spherical concave surfaces 1 and 2. This observation is experimentally and analytically achieved by Fenz and Constantinou (2008b). At first, sliding occurs on spherical innermost concave surfaces 2 and 3 then stops when sliding starts on outermost spherical concave surfaces 1 and 4. Then sliding starts on innermost surfaces 2 and 3 again when the outer concave plates contacts restrainer displacement. The mentioned motions are depicted in Fig. 2.

Schematic view of three SCFP bearing elements connected in series is shown in Fig. 3. In this figure, $1/\bar{R}_{effi}$, $\bar{\mu}_i$ and \bar{d}_i represent the stiffness of the spring based on the effective radius of curvature i ; the velocity dependent coefficient of friction and the displacement of the gap link element, respectively. Over bar notation is employed to symbolize parameters and responses related with the series model. In the other hand, normal notation is employed to symbolize parameters and responses related with the TCFP bearing.

In the series model, displacement of element i begins when horizontal force, F , exceeds the friction force. The friction force for each concave surface by means of $\bar{F}_{fi} = \bar{\mu}_i W$ where W is the vertical load acting on the bearing. Motion of i elements stops when i_{th} element displacement becomes equal to displacement capacity \bar{d}_i . This occurs at an applied horizontal force:

$$F_i = \frac{W}{R_{effi}} \bar{d}_i + \mu_i W \quad (1)$$

The force-displacement relationship can be obtained by considering the series model is depicted in Fig. 4. The model nearly gives the same actual force-displacement relationship which exhibits the TCFP bearing. The series model is recommended by Fenz and Constantinou (2008b). Fig. 4 shows how to create the series model of the TCFP bearing in SAP2000 is by assembling of three friction pendulum (FP) link elements, four gap link elements, and five rigid beam elements (RBE) in the finite element analysis.



Fig. 2 The possible positions of the TCFP bearing

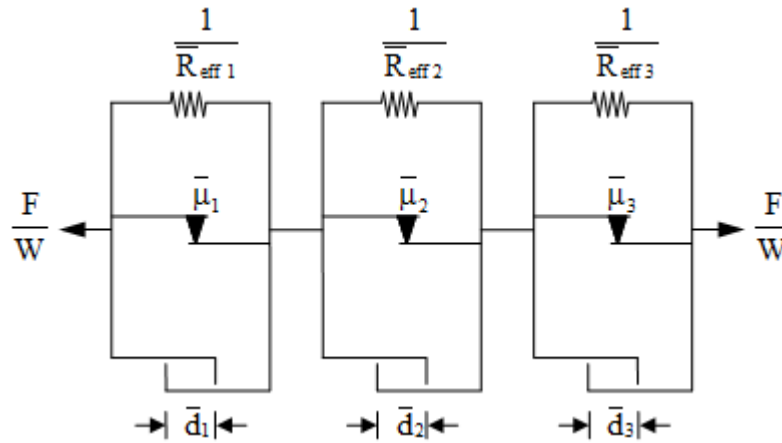


Fig. 3 The three SCFP elements in series model representing the TCFP bearing

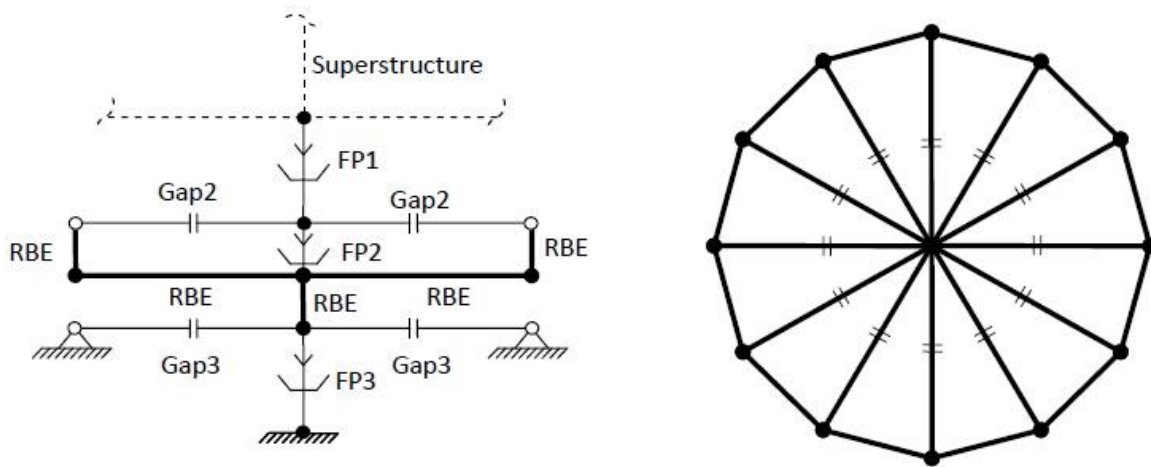


Fig. 4 3D-Series model of the TCFP bearing used in SAP2000

The arrangement described in the figure is exact only for horizontal excitation in one direction. One may be tempted to include gap elements in both orthogonal horizontal directions and perform a full three dimensional analysis. However, the results would be flawed because the gap element’s properties in SAP2000 are uncoupled; that is, they are independent in each deformational degree of freedom (SAP2000 2007). Physically, this represents a bearing that is square in plan. Obviously, the bearing is circular in plan, which means that the gap element must engage when the resultant relative displacement equals the displacement capacity \bar{d}_i . However, a coupled gap element is not currently available in SAP2000. To work around this, more gap elements can be used in the assembly to approximate a circle using straight line segments. Though the assembly becomes somewhat complex, the “*replicate radial*” command can be used to efficiently build the model. Alternatively, a preliminary analysis can be conducted without gap elements to determine the directions in which they would be engaged. The model can be modified to include gap elements in these directions (Fenz and Constantinou 2008b).

2.2 Formulation of the series model of the TCFP

In the series modeling scheme proposed by Fenz and Constantinou (2008b), the FP1 link element represents the combined behavior of inner surfaces 2 and 3, the FP2 link element represents the behavior of outer surface 1 and the FP3 link represents outer surface 4. Since there is no adjustment made to the vertical load supported by the bearings, to ensure that sliding initiates correctly for each element there are no modifications made to the coefficients of friction.

$$\bar{\mu}_1 = \mu_2 = \mu_3 \quad (2)$$

$$\bar{\mu}_2 = \mu_1 \quad (3)$$

$$\bar{\mu}_3 = \mu_4 \quad (4)$$

The actual behavior is sliding occurring only on surfaces 2 and 3. In the series model, sliding takes place only for FP1 link element:

$$\bar{R}_{eff1} = R_{eff2} + R_{eff3} \quad (5)$$

The effective radius of the FP2 link element in the series model is obtained by equating the stiffness given by the series model with the actual stiffness exhibited by the bearing:

$$\frac{W}{\bar{R}_{eff1} + \bar{R}_{eff2}} = \frac{W}{R_{eff1} + R_{eff3}} \quad (6)$$

and combining Eqs. (5) and (6), the effective radius for FP2 link element can be obtained as:

$$\bar{R}_{eff2} = R_{eff1} - R_{eff2} \quad (7)$$

The effective radius of FP3 link element in the series model is attained by equating the stiffness given by the series model with the actual stiffness exhibited by the bearing:

$$\frac{W}{\bar{R}_{eff1} + \bar{R}_{eff2} + \bar{R}_{eff3}} = \frac{W}{R_{eff1} + R_{eff4}} \quad (8)$$

by combining Eqs. (5), (7)-(8), the effective radius for the FP3 link element can be obtained as:

$$\bar{R}_{eff3} = R_{eff4} - R_{eff3} \quad (9)$$

In the series model, gap link elements are also used in order to achieve the true force-displacement relationship of the TCFP bearing. So, displacements at which the gap link element are given by following equations:

$$\bar{d}_2 = \frac{R_{eff1} - R_{eff2}}{R_{eff1}} d_1 \quad (10)$$

$$\bar{d}_3 = \frac{R_{eff4} - R_{eff3}}{R_{eff4}} d_4 \quad (11)$$

If desired to model the total displacement capacity of the bearing, the displacement capacity of the FP1 link element can be assigned as:

$$\bar{d}_1 = (d_1 + d_2 + d_3 + d_4) - (\bar{d}_2 + \bar{d}_3) \quad (12)$$

The rate parameter a is adjusted to properly model the velocity dependence of the coefficient of friction on outer surfaces 1 and 4. This is provided by indicating:

$$a_2 = \frac{R_{eff1}}{R_{eff1} - R_{eff2}} a_1 \tag{13}$$

$$a_3 = \frac{R_{eff4}}{R_{eff4} - R_{eff3}} a_4 \tag{14}$$

For FP1 link element of the series model, the rate parameter can be specified as half of the average of the rate parameters on surfaces 2 and 3 of the TCFP bearing. Therefore,

$$a_1 = \frac{a_2 + a_3}{4} \tag{15}$$

3. Numerical example

Gülburnu Highway Bridge located on the Giresun-Espiye state highway in Giresun, Turkey is selected for numerical example. The view of the bridge just before opening the traffic can be shown in Fig. 5. This bridge was constructed with balanced cantilever method using cast-in-place construction technique. The bridge deck consists of a main span of 165m and two side span of 82.5m each. The total bridge length is 330m and width of bridge is 30m. The structural system of the bridge consists of deck, columns and side supports is shown in Fig. 6. Some additional information about the bridge can be advisable from the literature (Altunisik et al. 2011).

This bridge actually seismically isolated with SCFP pendulum bearings. Eight FP isolators exist on the four columns. According to the project design criteria, earthquake isolation system has the ability of movement of 50cm. The cross section of friction pendulum system used in the Gülburnu Highway Bridge is shown in Fig. 7.

Three dimensional FEM of the bridge is constructed using SAP2000 software (Fig. 8). In the FEM; deck, columns and bored piles are modeled by frame elements, raft foundations are modeled as shell elements. To determine and compare the analyses results, dynamic earthquake responses of the bridge are attained by using of three different FEM considering non-isolated column-deck interaction, SCFP system and TCFP system between column and deck. The selected material properties of the bridge used in analysis are given in Table 1.

The ERZ-EW and ERZ-NS components of 1992 Erzincan earthquake ground motion are used in the dynamic analysis to determine the structural responses of the bridge (PEER 2012). This earthquake has a magnitude value as 6.8 ($M_w=6.8$). The EW and NS components of earthquake ground motion are applied to the bridge at the longitudinal and transverse directions, respectively. The acceleration of gravity is also included in the vertical component by using a ramp function in the beginning of the time history in order to take into account the effect of the dead load on the behavior of the TCFP bearings. The actual properties of TCFP bearing system are given in Table 2.

The important and essential parameters for modelling of the bridge using TCFP bearing as a series model in SAP2000 software are given in Table 3. These parameters are obtained from Table 2 using some special equations (Fenz and Constantinou 2008b, Fenz 2008, Yurdakul and Ates 2011, Ates and Yurdakul 2011). The modal analyses of all FEM (non-isolated column-deck interaction, SCFP system and TCFP system between column and deck) are performed and dynamic characteristics are determined. The first five periods are presented in Table 4 to determine



Fig. 5 Some views of Gülburnu Highway Bridge

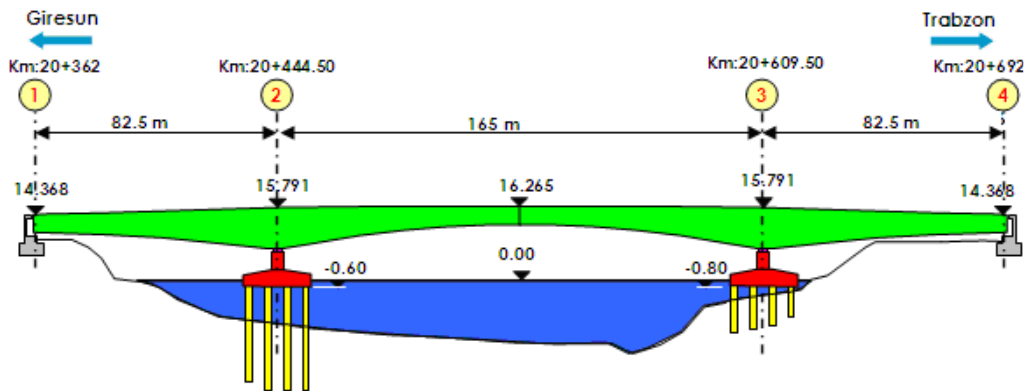


Fig. 6 Basic configuration of Gülburnu Highway Bridge (Yüksel Project 2007)

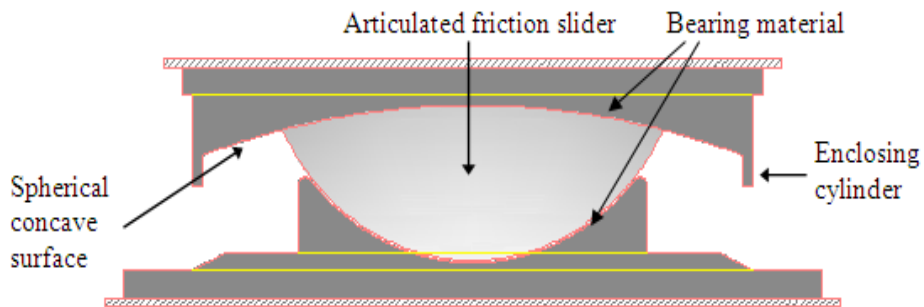


Fig. 7 The cross-section of the friction pendulum system (Yüksel Project 2007)

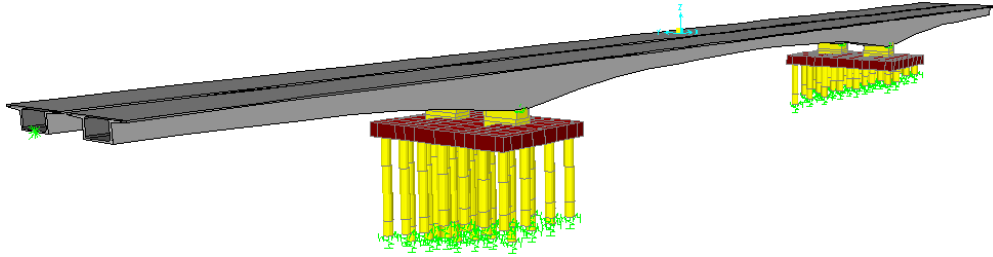


Fig. 8 FEM of Gülburnu Highway Bridge

Table 1 Properties of the materials considered in finite element analyses

Elements	Class	Modulus of Elasticity (kN/m ²)	Poisson ratio (-)	Density (kg/m ³)
Decks	C40	3.60E07	0.2	2500
Abutments	C35	3.50E07	0.2	2500
Piers	C30	3.40E07	0.2	2500
Base	C30	3.40E07	0.2	2500
Reinforcement*	S420	2.10E08	0.2	7850

*Yield stress=1600MPa Ultimate stress=1860MPa

Table 2 Actual properties of the TCFP bearing

Name of the Property	Values
$R_{eff1}=R_{eff4}$ (mm)	2108.2
$R_{eff2}=R_{eff3}$ (mm)	203.2
$d_1=d_4$ (mm)	345.0
$d_2=d_3$ (mm)	170.0
$\mu_1=\mu_4$	0.05
$\mu_2=\mu_3$	0.025

Table 3 The parameters of the series model for TCFP bearing

Element height (mm)	300	270	270
Shear deformation location (mm)	150	135	135
Supported weight (kN)	38000	38000	38000
Vertical stiffness (kN/m)	274900	274900	274900
Elastic stiffness (kN/m)	475	950	950
Effective stiffness (kN/m)	93504	19948	19948
Friction coefficient-fast	0.025	0.050	0.050
Friction coefficient-slow	0.0125	0.025	0.025
Radius (mm)	406.4	1.905	1.905
Rate parameter (sec/mm)	0.025	0.550	0.550
Gap element (mm)	-----	312	312

Table 4 The first main periods obtained from the analysis

Mode Number	Non-isolated (sec)	SCFP (sec)	TCFP (sec)
1	1.178	2.012	2.963
2	1.085	1.915	2.962
3	0.980	1.875	2.141
4	0.849	1.778	2.139
5	0.627	1.404	1.411

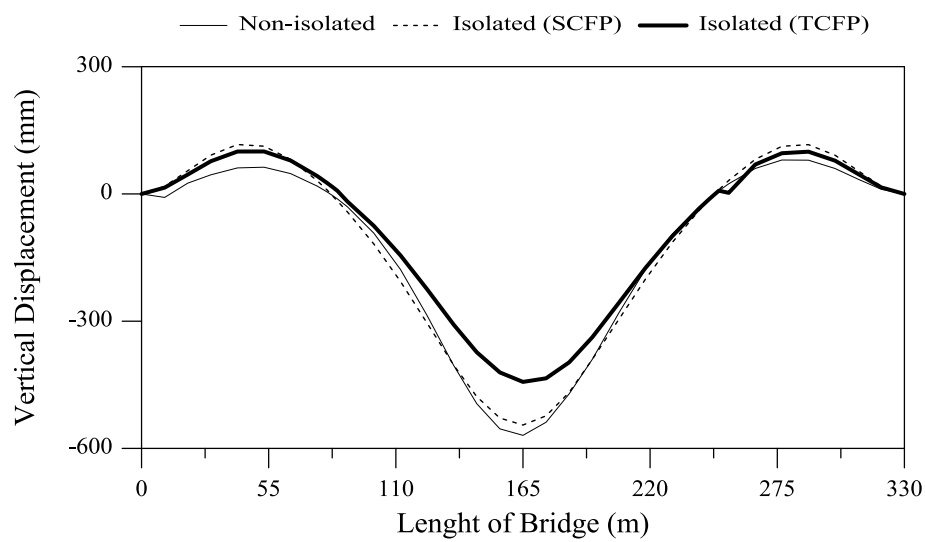


Fig. 9 Changing of maximum vertical displacements along the bridge deck

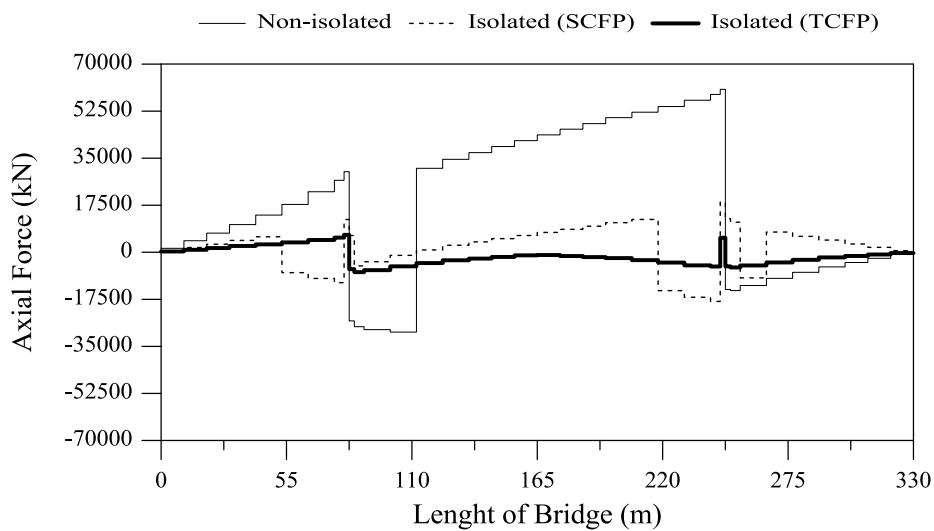


Fig. 10 Changing of maximum axial forces along the bridge deck

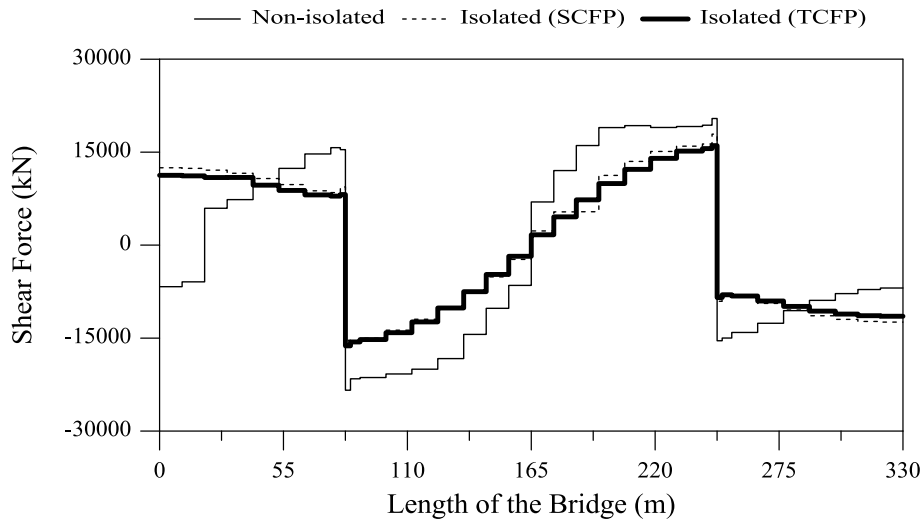


Fig. 11 Changing of maximum shear forces along the bridge deck

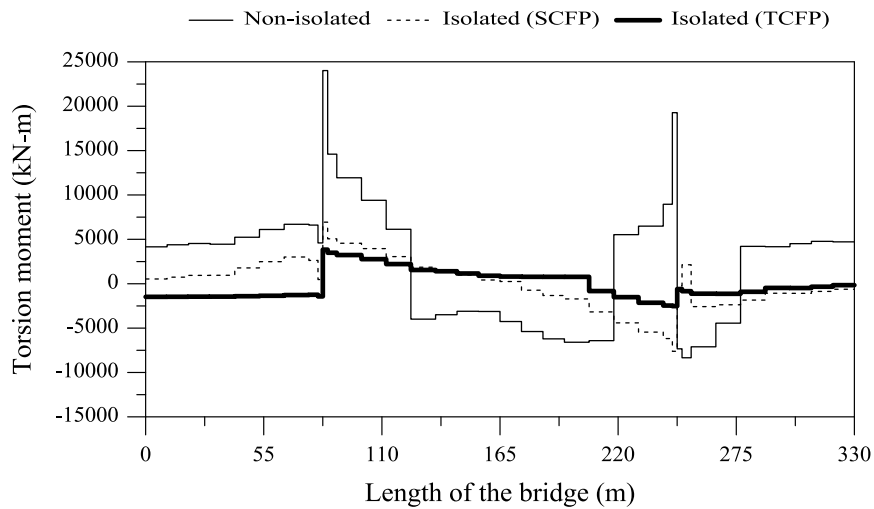


Fig. 12 Changing of maximum torsional moments along the bridge deck

the differences. It is seen that the periods have an increasing trend with using of single and TCFP. The first main periods increased from 1.178 sec (0.849Hz) to 2.012 sec (0.497Hz) and 2.963 sec (0.338Hz), respectively.

At the end of the analysis, displacements and internal forces are chosen as comparison parameters. The changing of vertical displacements, axial forces, shear forces and torsional moments obtained from non-isolated bridge, isolated bridge with SCFP and isolated with TCFP are given in Figs. 9-12, respectively. It is seen from the Fig. 9 that the displacements have an increasing trend along to the bridge span for all analyses conditions. The maximum vertical displacements are obtained as 57cm, 54cm and 44cm for non-isolated, isolated with SCFP and

isolated with TCFP conditions, respectively. It can be seen that TCFP system has an important and positive effect on the vertical displacements.

It is seen from the Fig. 10 that the axial forces have an increasing trend at the two side spans and main span, decreasing trend on the first and second columns. Maximum axial forces are obtained as 60619kN, 18728kN and 7382kN for non-isolated, isolated with SCFP and isolated with TCFP conditions, respectively. It can be seen that the values of axial forces decreased substantially with using of base isolation systems and TCFP system is a one of the best solution for structural design of long span highway bridges.

It is seen from the Fig. 11 that the shear forces have an increasing trend at the main span, but there isn't any distribution (increasing/decreasing) at the two side span. Maximum shear forces are obtained as 23408kN, 17913kN and 16249kN for non-isolated, isolated with SCFP and isolated with TCFP conditions, respectively. It can be seen that the values of shear forces decreased substantially with using of base isolation systems. Also, it is observed that the using of SCFP or TCFP system have same effects on the structural response. For these reasons, it is advised that SCFP or TCFP systems are one of the best solutions for structural design of long span highway bridges.

It is seen from the Fig. 12 that the torsional moments have an increasing trend along to the main columns and decreasing trend along the middle points of the deck. Maximum torsional moments are obtained as 24020kNm, 7619kNm and 3840kNm for non-isolated, isolated with SCFP and isolated with TCFP conditions, respectively. It can be seen that the values of torsional moments decreased substantially with using of base isolation systems and TCFP system is a one of the best solution for structural design of long span highway bridges.

4. Conclusion

In this paper, it is aimed to determine and compare the structural dynamic response of base isolated long span highway bridge using single and triple concave friction pendulums. Gülburnu Highway Bridge is selected as an application. The bridge is seismically isolated in the design phase. 3D FEM of the bridge is constituted using project drawings by SAP2000 software. Comparing the results of this study, the following observations can be made

- This bridge actually seismically isolated with SCFP pendulum bearings. Eight FP isolators exist on the four columns. According to the project design criteria, earthquake isolation system has the ability of movement of 50cm.
- The FEM of the bridge is constructed using SAP2000. The deck, columns and bored piles are modeled by frame elements, raft foundations are modeled as shell elements. To determine and compare the analyses results, dynamic earthquake responses of the bridge are attained by using of three different FEM considering non-isolated column-deck interaction, SCFP system and TCFP system between column and deck.
- The modal analyses of all FEM (non-isolated column-deck interaction, SCFP system and TCFP system between column and deck) are performed and dynamic characteristics are determined. It is seen that the periods have an increasing trend with using of SCFP and TCFP. The first main periods increased from 1.178 sec (0.849Hz) to 2.012 sec (0.497Hz) and 2.963 sec (0.338Hz), respectively. The increasing of periods provided the reduction of acceleration originates due to the earthquake. It's mean that the bridge can be resistant under severe

earthquakes.

- It is seen from the analyses that the displacements have an increasing trend along to the bridge span for all analyses conditions. The maximum vertical displacements are obtained as 57cm, 54cm and 44cm for non-isolated, isolated with SCFP and isolated with TCFP conditions, respectively. It can be seen that TCFP system has an important and positive effect on the vertical displacements. The maximum vertical displacement reduction between isolated with TCFP bearing and non-isolated bridge is %30. The maximum vertical displacement reduction between isolated with TCFP bearing and isolated with SCFP bearing bridge is %23. Also, the maximum vertical displacement reduction between isolated bridge using SCFP bearing and non-isolated bridge is 9%. It is deducted that the effective size of diameter has similar trend on vertical displacements because of its geometric shape.

- It is seen from the analyses that the axial forces have an increasing trend at the two side spans and main span, decreasing trend on the first and second columns. Maximum axial forces are obtained as 60619kN, 18728kN and 7382kN for non-isolated, isolated with SCFP and isolated with TCFP conditions, respectively. The maximum axial force reduction between isolated with TCFP bearing and non-isolated bridge is %88. The maximum axial force reduction between isolated with SCFP bearing and non-isolated bridge is %69. The maximum axial force reduction between isolated with TCFP bearing and isolated with SCFP bearing is %61. It can be seen that the values of axial forces decreased substantially with using of base isolation systems and TCFP system is a one of the best solution for structural design of long span highway bridges.

- It is seen from the analyses that the shear forces have an increasing trend at the main span, but there isn't any distribution (increasing/decreasing) at the two side span. Maximum shear forces are obtained as 23408kN, 17913kN and 16249kN for non-isolated, isolated with SCFP and isolated with TCFP conditions, respectively. The maximum shear force reduction between isolated with TCFP bearing and non-isolated bridge is %31. The maximum shear forces reduction between isolated with SCFP bearing and non-isolated bridge is %23. The maximum shear forces reduction between isolated with TCFP bearing and isolated with SCFP bearing is %9. It can be seen that the values of shear forces decreased substantially with using of base isolation systems. Also, it is observed that the using of SCFP or TCFP system has same effects on the structural response. For these reasons, it is advised that SCFP or TCFP systems are one of the best solutions for structural design of long span highway bridges.

- It is seen from the analyses that the torsional moments have an increasing trend along to the main columns and decreasing trend along the middle points of the deck. Maximum torsional moments are obtained as 24020kNm, 7619kNm and 3840kNm for non-isolated, isolated with SCFP and isolated with TCFP conditions, respectively. The maximum torsional moment reduction between isolated with TCFP bearing and non-isolated bridge is %84. The maximum torsional moment reduction between isolated with SCFP bearing and non-isolated bridge is %68. The maximum torsional moment reduction between isolated with TCFP bearing and isolated with SCFP bearing is %50. It can be seen that the values of torsional moments decreased substantially with using of base isolation systems and TCFP system is a one of the best solution for structural design of long span highway bridges.

- In TCFP, there is no sliding at all of the system under service loads. The sliding only occur internal concave plates. This increase life spans of system and reduces maintenance costs of the structures.

This study demonstrated that seismically isolated Gülburnu Highway Bridge with TCFP

bearings has minimum displacements and internal forces responses as against the non-isolated and SCFP models. The decrease between FEM of the bridge with TCFP bearing system and FEM of the bridge with SCFP bearing system is %19, %60, %9, and %50 for vertical displacement, axial force, shear force, and torsional moment, respectively.

References

- Altunisik, A.C., Bayraktar, A., Sevim, B. and Ates, S. (2011), "Ambient vibration based seismic evaluation of isolated gülburnu highway bridge", *Soil Dyn. Earthq. Eng.*, **31**(11), 1496-1510.
- Ates, S. and Constantinou, M. (2011), "Example of application of response spectrum analysis for seismically isolated curved bridges including soil-foundation effects", *Soil Dyn. Earthq. Eng.*, **31**(4), 648-661.
- Ates, S. and Yurdakul, M. (2011), "Site-response effects on rc buildings isolated by triple concave friction pendulum bearings", *Comput. Concr.*, **8** (6), 693-715.
- Brownjohn, J.M.W., Magalhaes, F., Caetano, E. and Cunha, A. (2010), "Ambient vibration re-testing and operational modal analysis of the humber bridge", *Eng. Struct.*, **32**(8), 2003-2018.
- Computers and Structures Inc. (2007), *SAP2000: Static and Dynamic Finite Element Analysis of Structures*, Berkeley, CA, USA.
- Dicleli, M. and Mansour, M.Y. (2003), "Seismic retrofitting of highway bridges in illinois using friction pendulum seismic isolation bearings and modelling procedures", *Eng. Struct.*, **25**(9), 1139-1156.
- Dicleli, M., Albhaisi, S. and Mansour, M.Y. (2005), "Static soil-structure interaction effects in seismic-isolated bridges", practice periodical on structural design and construction, ASCE, **10** (1), 22-33.
- Fenz, D.M. and Constantinou, M.C. (2008a), "Spherical sliding isolation bearings with adaptive behavior: theory", *Earthquake Engineering and Structural Dynamics*, **37**(2), 163-183.
- Fenz, D.M. and Constantinou, M.C. (2006), "Behavior of the double concave friction pendulum bearing", *Earthq. Eng. Struct. Dyn.*, **35**(11), 1403-1424.
- Fenz, D.M. and Constantinou, M.C. (2008b), "Modeling triple friction pendulum bearings for response history analysis", *Earthq. Spectra*, **24**(4), 1011-1028
- Fenz, D.M. (2008), "Development, implementation verification of dynamic analysis models of multi-spherical sliding bearings", Ph.D. Dissertation, State University of New York at Buffalo, New York.
- Hamidi, M., Naggar, M.H.E., Vafai, A. and Ahmadi, G. (2003), "Seismic isolation of buildings with sliding concave foundation (SCF)", *Earthq. Eng. Struct. Dyn.*, **32**(1), 15-29.
- Hyakuda, T., Saito, K., Matsushita, T., Tanaka, N., Yoneki, S., Yasuda, M., Miyazaki, M., Suzuki, A. and Sawada, T. (2001), "The structural design and earthquake observation of a seismic isolation building using friction pendulum system", In: *Proceedings of the 7th international seminar on seismic isolation, passive energy dissipation and active control of vibrations of structures*, Assisi, Italy, October.
- Jangid, R.S. (2004), "Seismic response of isolated bridges", *J. Bridge Eng.*, **9** (2), 156-166.
- Kelly, J.M. (1997), "Earthquake resistant design with rubber", Berlin, Heidelberg, NY: Springer-Verlag.
- Tsopelas, P. and Constantinou, M.C. (1996), "Experimental study of fps system in bridge seismic isolation", *Earthq. Eng. Struct. Dyn.*, **25**(1), 65-78.
- Madhekar, S.N. and Jangid, R.S. (2010), "Seismic performance of benchmark highway bridge with variable friction pendulum system", *Adv. Struct. Eng.*, **13** (4), 561-589.
- Marin-Artieda, C.C. and Whittaker, A.S. (2010), "Theoretical studies of the XY-FP seismic isolation bearing for bridges", *J. Bridge Eng.*, **15**(6) 631-638.
- PEER: Pacific Earthquake Engineering Research Centre.
<http://peer.berkeley.edu/smcat/data/ath/SFERN/PCD.AT2>; 2012
- Rahman Bhuiyan, A. and Shahria Alam, M. (2013), "Seismic performance assessment of highway bridges equipped with superelastic shape memory alloy-based laminated rubber isolation bearing", *Eng. Struct.*, **49**, 396-407.

- Soni, D.P., Mistry, B.B., Jangid, R.S. and Panchal, V.R. (2011), "Seismic response of double variable frequency pendulum isolator", *Struct. Control Health Monit.*, **18**(4) 450-470.
- Yurdakul, M. and Ates, S. (2011), "Modeling of triple concave friction pendulum bearings for seismic isolation of buildings", *Struct. Eng. Mech.*, **40** (3), 315-334.
- Yüksel Project. (2007), "Gülburnu bridge-detailed design".

CC